RSC Advances

ROYAL SOCIETY OF CHEMISTRY

www.rsc.org/advances

Cite this: DOI: 10.1039/c0xx00000x

www.rsc.org/xxxxxx

ARTICLE TYPE

Two Keggin sandwich-type tungstophosphates modified by open-chain carboxyethyltin groups and transition metals

Bai Zhang,[a] Lan-Cui Zhang,*[a] Ya-Jun Zhang,[a] Fang Su,[a,b] Wan-Sheng You*[a] and Zai-Ming Zhu*[a]

Received (in XXX, XXX) Xth XXXXXXXXX 20XX, Accepted Xth XXXXXXXXX 20XX

DOI: 10.1039/b000000x

Two new polyoxometalates containing $[PW_9O_{34}]^{9-}$ (Abbreviated as **PW_9**) subunits, carboxyltin groups and transition metal ions, namely $K_{10}[Mn_2\{Sn(CH_2)_2COO\}_2[(B\text{-}\alpha\text{-}PW_9O_{34})_2]\cdot 14H_2O$ (**1**) and $Na_8K_2[Zn_2\{Sn(CH_2)_2COO\}_2[(B\text{-}\alpha\text{-}PW_9O_{34})_2]\cdot 13H_2O$ (**2**), were successfully assembled in aqueous solutions by routine synthetic method, and fully characterized. They represent the first single crystal examples of open -chain carboxyethyltin group-modified Keggin sandwich-type tungstophosphates. Their important structural features are that two open-chain carboxyethyltin moieties attached on the **PW_9** dimer, forming arm-type polyoxometalates. Furthermore, the fluorescence properties, electrocatalytic and oxidation catalytic activities were evaluated. More interestingly, the fluorescence quenching of **1**/**2**-doped TiO_2 was clearly observed, which means that the two compounds may be excellent components of photocatalytic materials.

Introduction

In recent decades, polyoxometalates (POMs) have been found widespread applications in many fields owing to their structural diversities and remarkable properties.[1] Earlier works demonstrated that organotin groups can be introduced into the skeletons of polyoxoanions due to the stability of the Sn−C bond and the similar sizes of Sn (IV) and W(VI).[2] In 1994, Pope et al. firstly synthesized a new sandwich-type tungstophosphate decorated by three PhSnOH groups.[3] Since then, organotin-decorated POMs, have been received increasing attention. Most of these research work are mainly concentrated on the use of alkyltin groups, some POMs modified by dimethyltin, phenyltin and butyltin groups were reported.[2b,4-6] Compared with the aforementioned compounds, the estertin or carboxyethyltin group modified lacunary POMs were rarely reported.[7] Because the estertin compounds are susceptible to hydrolysis in a POM system, and it is difficult to obtain single crystal POM-estertin derivatives. Within the class of organotin groups, estertin or carboxyethyltin compounds have broad applications on the basis of low-toxicity, higher thermal stability,[8] such as catalysis, antiviral and antitumor agents, and various functional materials.[7c,9-11] In 2010, we obtained the first tetra(carboxyethyltin)-decorated POM confirmed by single crystal X-ray diffraction and NMR analysis.[12] To date, some crystalline examples of cyclic carboxyethyltin decorated POMs have been reported by our team[13]. It is found that carboxyltin moieties as better functional groups can enhance the POM′s properties and will give their new applications. Delightedly, the POM-estertin derivatives are good photoelectric materials, *e.g.* our previously reported sandwich-type tungstogermanates with open-chain carboxyltin groups displayed the primary features of sensitizers in DSSCs,[14] and they could markedly increase the electrocatalytic activity of single-walled carbon nanotube toward triiodide reduction when assembled into composite electrodes.[15] Such novel sandwich-type POMs now have attracted our strong interest and desirable exploration. As a continuation of our recent research work, in the present study, we obtained two Keggin sandwich-type tungstophosphates decorated by two open-chain carboxyltin groups, $K_{10}[Mn_2\{Sn(CH_2)_2COO\}_2[(B\text{-}\alpha\text{-}PW_9O_{34})_2]\cdot 14H_2O$ (**1**) and $Na_8K_2[Zn_2\{Sn(CH_2)_2COO\}_2[(B\text{-}\alpha\text{-}PW_9O_{34})_2]\cdot 13H_2O$ (**2**). Both compounds exhibit arm-type structures, in which two Mn^{2+}/Zn^{2+} cations and two open-chain carboxyethyltin groups were sandwiched between B-α-$[PW_9O_{34}]^{9-}$ units.

Experimental

Materials and methods

$K_{10}[Mn_4(H_2O)_2(PW_9O_{34})_2]\cdot 41H_2O$, $K_{10}[Zn_4(H_2O)_2(PW_9O_{34})_2]\cdot 22H_2O$ (Abbreviated as **PW_9-Mn** and **PW_9-Zn**) and $Cl_3Sn(CH_2)_2COOCH_3$ were synthesized according to the literatures and characterized by IR spectra.[16-18] All other chemicals were purchased commercially and used without further purification. C and H elemental analyses were performed on a Vario Elcube elemental analyzer, and P, Sn, Mn, Zn and W were analyzed on a Prodigy XP emission spectrometer. X-ray diffraction data were collected on a Bruker Smart APEX II X-diffractometer equipped with graphite-monochromated Mo Kα radiation (λ = 0.71073 Å). IR spectra were recorded in the range of 4000-400 cm^{-1} on a Bruker AXS TENSOR-27 FT-IR spectrometer using KBr pellets. TG analyses were performed on a Pyris Diamond TG/DTA instrument in an air atmosphere with a heating rate of 10 °C min^{-1}. NMR spectra were recorded at room temperature with a 500 MHz Bruker AVANCE 500 spectrometer.

An inner tube containing D_2O was used as an instrumental lock. Phosphorus and tin chemical shifts were referenced to 85% H_3PO_4 and $(CH_3)_4Sn$, respectively. Electrochemical measurements were carried out on a CHI 604B electrochemical workstation at room temperature. The working electrode was the glassy carbon electrode. A platinum wire was used as the counter electrode and a Ag/AgCl (3 mol L^{-1} KCl) was the reference electrode. The concentration of compounds **1** and **2** were 1.0×10^{-4} mol L^{-1}. The yield of cyclohexanone was confirmed on a JK-GC112A Gas Chromatograph. The photoluminescence property was determined on a RILI F-7000 fluorescence spectrophotometer in the solid state at room temperature.

Synthetic procedures

Synthesis of 1. $Cl_3Sn(CH_2)_2COOCH_3$ (0.15 g, 0.50 mmol) was dissolved in 10.0 mL H_2O to form solution A, and **PW_9-Mn** (1.46 g, 0.25 mmol) was dissolved in 10.0 mL H_2O to form solution B. Then, solution A was added dropwise to solution B. The resulting solution was stirred at 80 °C for about 2 h, and then cooled to room temperature. Subsequently, 3.00 g of KCl was added into the above solution, after filtration, the filtrate was slowly evaporated at 50 °C. Yellow block crystals of **1** was isolated after five days (yield 32% based on W), Elemental analysis, Found: C, 1.27; H, 0.63; P, 1.13; K, 7.08; Sn, 4.26; Mn, 1.96; W, 59.14. Calc. for $C_6H_{36}K_{10}Mn_2O_{86}P_2Sn_2W_{18}$: C, 1.29; H, 0.65; P, 1.11; K, 6.99; Sn, 4.24; Mn, 1.96; W, 59.16%. FT IR (KBr pellet), cm^{-1}: 3487(s), 2904(w), 2842(w), 1623(m), 1396(w), 1226(w), 1037(m), 948(s), 875(m), 763(s), 493(w), 420(w) cm^{-1}.

Synthesis of 2. The synthetic method of **2** was similar to that of **1**, only **PW_9-Mn** was replaced by **PW_9-Zn** (1.39 g, 0.25 mmol). Colourless block crystals of **2** was isolated after six days (yield 39% based on W), Elemental analysis, Found: C, 1.36; H, 0.68; P, 1.13; K, 1.47; Na, 3.39; Sn, 4.31; Zn, 2.44; W, 60.60. Calc. for $C_6H_{34}K_2Na_8Zn_2O_{85}P_2Sn_2W_{18}$: C, 1.32; H, 0.63; P, 1.13; K, 1.43; Na, 3.36; Sn, 4.34; Zn, 2.39; W, 60.52%. FT IR (KBr pellet), cm^{-1}: 3438(m), 2933(w), 2842(w), 1620(m), 1389(m), 1047(m), 956(s), 884(m), 764(s), 499(w) cm^{-1}.

Preparation of 1, 2, PW_9-Mn/Zn loaded TiO_2. **1/2** or **PW_9-Mn/Zn** (0.5 g) was dissolved in 20 mL distilled water, and to this aqueous solution was added TiO_2 (2.8 g) with stirring. After 2 h at 90 °C, the target products, denoting as **1-TiO_2, 2-TiO_2**, **PW_9-Mn-TiO_2** and **PW_9-Zn-TiO_2**, were dried in an oven at 120 °C.

X-ray crystallography

The structures were solved by direct methods and refined by full-matrix least-squares fitting on F^2 using SHELXTL-97 package.[19] An empirical absorption correction was applied using the SADABS program. Cell parameters were obtained by the global refinement of the positions of all collected reflections. All the non-hydrogen atoms were refined anisotropically. Hydrogen atoms on C atoms were added in calculated positions. Crystal data and structure refinement parameters of compounds **1** and **2** are listed in Table 1. Selected bond lengths and angles are given in Tables S1, S2.† CCDC reference numbers: 1060303, 1060304.

Catalytic tests

Electrocatalytic activities. The electrocatalytic study was conducted in pH = 3 (0.1 mol L^{-1} Na_2SO_4-H_2SO_4) solution at room temperature. The concentration of H_2O_2 was 0-2 mmol L^{-1}.

Table 1 Crystal and refinement data for compounds **1** and **2**

compound	**1**	**2**
Formula	$C_6H_{36}K_{10}Mn_2O_{86}P_2Sn_2W_{18}$	$C_6H_{34}K_2Na_8Zn_2O_{85}P_2Sn_2W_{18}$
formula weight	5593.85	5467.81
Crystal system	Triclinic	Triclinic
Space group	$P\bar{1}$	$P\bar{1}$
a / Å	12.3609(6)	12.2118(17)
b/ Å	12.3687(6)	12.401(2)
c/ Å	16.1134(8)	15.826(2)
α /°	80.798(1),	96.179(3)
β /°	81.685(1),	104.324(2)
γ /°	67.547(1)	119.353(2)
V / Å^3, Z	2238.05(19), 1	1948.2(5), 1
T / K	296(2)	296(2)
Wavelength / Å	0.71073	0.71073
D_c / g·cm^{-3}, F_{000}	4.150, 2462	4.660, 2398
Reflections collected	11403	9870
R_{int}	0.0297	0.0575
θ /°	1.79 - 25.00	1.93 - 25.00
GOF	1.048	1.027
R_1 ($I > 2\sigma(I)$)	0.0410	0.0770
wR_2 (all data)[a]	0.1180	0.2194

[a] $R_1 = \sum||F_0|-|F_C||/\sum|F_0|$; $wR_2 = \sum[w(F_0^2-F_C^2)^2]/\sum[w(F_0^2)^2]^{1/2}$

The electrocatalytic activity of **1/2** toward the reduction of hydrogen peroxide could be evaluated by the peak current changes in the CV curves.

Oxidation of cyclohexanol to cyclohexanone. Following the method mentioned in our previous work,[13b] the typical procedure for the oxidation catalytic synthesis is: the catalyst (**1/2**) was added to a mixture of cyclohexanol and acetonitrile in a 100 mL three-necked round-bottom flask equipped with a reflux condenser, and 30% H_2O_2 was dropwise added to the mixture under refluxing conditions (*ca.* 80 °C) over 2 h. After completing the reaction, the solvent acetonitrile was removed by distillation, and thus the organic and inorganic phases could be separated by separatory funnel extraction method, and the catalyst was remained in the reaction vessel. Additionally, the reusabilities of compounds **1** and **2** were studied through four cycles under optimum reaction conditions. The products obtained were characterized by gas chromatography.

Results and discussion

Synthesis

Although the crystalline POM-estertin derivatives are difficult to obtain, our experiments showed that the carboxyltin group can be introduced into the POM systems, such as lancunary keggin-type, Dawson-type POMs. For example, **PW_9** is one of good building block, it can react with estertin $Cl_3Sn(CH_2)_2COOCH_3$ in aqueous solution, meanwhile some transition metal ions can also join the POM framework. Surprisingly, we found that the type and configuration of POM precursor, including the transition metal can directly affect the configuration of the carboxyltin in the products. In our previous work, we selected A-α-**PW_9** and $[Sn(CH_2)_2COOCH_3]^{3+}$ as inorganic and organic precursors, respectively, the final product was a sandwich-type POM (A-α-**PW_9-SnR**) containing cyclic carboxyethyltin $[Sn(CH_2)_2COO]^{2+}$ moieties (See Scheme 1, step I).[13b] While in the present work, the inorganic precursor was sandwich-type **PW_9-Mn** or **PW_9-Zn** based on B-α-**PW_9** subunit, the configuration of the carboxyltin

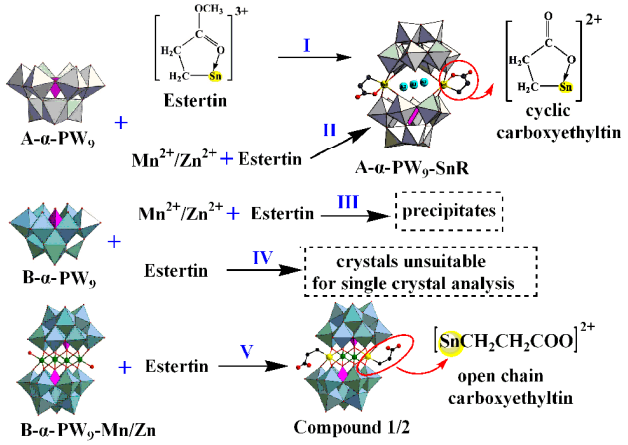

Scheme 1 Schematic representation of the formations of Keggin sandwich-type tungstophosphates containing cyclic and open chain carboxyltin groups

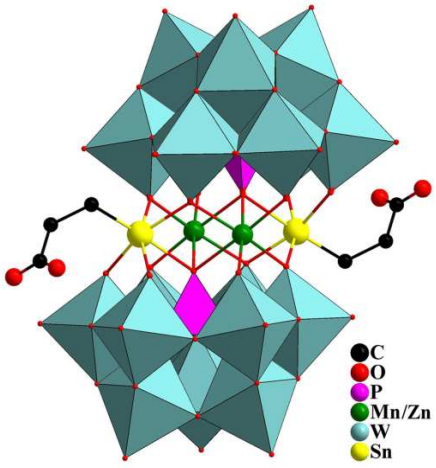

Fig. 1 Polyhedral and ball-and-stick representation of the polyoxoanion in **1** and **2**

in the final product was not the same as that of the former, as shown in Scheme 1 (step V), two transition metal ions were replaced by two carboxyethyltin groups. Furthermore, the cyclic carboxyltin has converted into the open chain structure $[Sn(CH_2)_2COO]^{2+}$. When we selected B-α-**PW$_9$** unit and Mn^{2+}/Zn^{2+} as inorganic precursors, we failed to obtain crystalline **1** or **2** (Scheme 1, step III), although we try to change the addition order and proportion of the reactants. If the transition metal and carboxyltin ions were added into the A-α-**PW$_9$** system (Scheme 1, step II), the product was A-α-**PW$_9$-SnR** as the same as step I, Which may be due to the fierce competition between the inorganic metal and organometallic ions. Moreover, the pH value is one of the key factors to the synthesis, and the optimum pH value is about 4−6.

Crystal structure

Single crystal X-ray diffraction analysis reveals that the isostructural polyoxoanion of **1**/**2** displays the well-known Keggin sandwich-type structural feature (Fig. 1). Its symmetrical unit consists of a B-α-**PW$_9$** subunit modified by Mn^{2+}/Zn^{2+} and one carboxyethyltin group (Fig. S1†). The central core of the polyanion contains two open-chain $[Sn(CH_2)_2COO]^{2+}$ moieties and two MnO_6/ZnO_6 fragments located in the outer and inner positions, respectively. In **1** or **2**, each Sn atom coordinates with five oxygen atoms from two B-α-**PW$_9$** subunits and one carbon atom from a $[Sn(CH_2)_2COO]^{2+}$ group. Each Mn^{2+} or Zn^{2+} ion is six-coordinated by six terminal oxygen atoms derived from two B-α-**PW$_9$** units. The bond lengths of Sn−O are in the range of 2.070(10)-2.403(9) and 2.00(2)-2.321(17) Å, and the Sn−C are 2.155(13) and 2.10(2) Å for **1** and **2**, respectively. The Mn−O and Zn−O distances are in the range of 2.052(10)-2.328(9) and 2.00 (2)-2.287(17) Å, respectively. The W−O distances are in the range of 1.703(10)-2.601(9) and 1.69(2)-2.574(17) Å for **1** and **2**, respectively. Wherein three WO_6 octahedra in **1** obviously distorted with longer W−O bonds (W2−O16 2.574, W5−O11 2.535, W9−O13 2.601). In **2**, there is one longer W−O bond (W4−O22 2.574). Furthermore, the estertin precursor $[Sn(CH_2)_2COOCH_3]^{3+}$ also hydrolyzed into the carboxyethyltin $[Sn(CH_2)_2COO]^{2+}$ during the reaction process. Interestingly, the cyclic carboxyethyltin converted into a chain structure, due to the original Sn−$O_{carboxyl}$ bond is broken. The open-chain carboxyl-terminal group can link with metal cations or organic groups, that is to say, the exposed carboxyl group (–COO) may advantageously be further functionalized. In the packing arrangement of **1** or **2**, the adjacent sandwich-type polyoxoanions are stacked into a 3D supramolecular framework *via* the extensive H-bonding interactions between water molecules and the polyoxoanions, as well as the electrostatic forces between Na^+/K^+ cations and polyoxoanions (Fig. S2†).

Characterization

FT-IR spectroscopy. IR spectra of compounds **1** and **2** are similar (Fig. S3 and S4†). The peaks between 1030 and 760 cm^{-1} are assigned to the characteristic vibrations of POMs, the peaks at 948, 875, 763 cm^{-1} for **1** and 956, 884, 764 cm^{-1} for **2** are attributed to the asymmetric stretching vibrations of the terminal (W−O_t) and bridge (W−$O_{b,c}$−W) bonds (O_t and O_b/O_c terminal and bridging O atoms). The P−O stretching is at about 1037, 1047 cm^{-1}, respectively.[13,20] The peaks at 420, 493 and 628 cm^{-1} for **1** are assigned to the stretching vibration of Sn−O bond, the antisymmetric and symmetric vibrations of Sn−C bonds, respectively. While for **2**, the weak peaks of Sn−O and symmetric vibration of Sn−C bond vibrations are overlapped, only the antisymmetric vibration (493 cm^{-1}) of Sn−C bond is observed. The peaks at 2904, 2842 and 1396 cm^{-1} for **1** and 2933, 2842 and 1389 cm^{-1} for **2** are attributed to the characteristic vibrations of the organic group (−CH_2). The ν_{as}(COO) and ν_s(COO) vibrations appear at 1623, 1226 and 1620, 1222 cm^{-1} for **1** and **2**, respectively.[12,21]

X-ray power diffraction. The powder XRD patterns of compounds **1** and **2** and their simulated XRD patterns are shown in Figs. S5 and S6.† The diffraction peaks on the pattern correspond well in position, confirming that the product is a pure phase. The differences in reflection intensity are probably due to preferred orientation in the powder samples.

Thermal analysis. The thermal stabilities of compounds **1** and **2** were measured in the range of 35 to 1000 °C. As shown in Fig. S7,† the TG curve of compound **1** shows three continuous weight loss steps from 35 to 660 °C. The total weight loss of 6.97% (Calc. 7.09%) corresponds to the loss of all lattice water molecules and the removal of two $(CH_2)_2COO$ groups. For compound **2**, it has similar thermal stability to **1**. In the range of

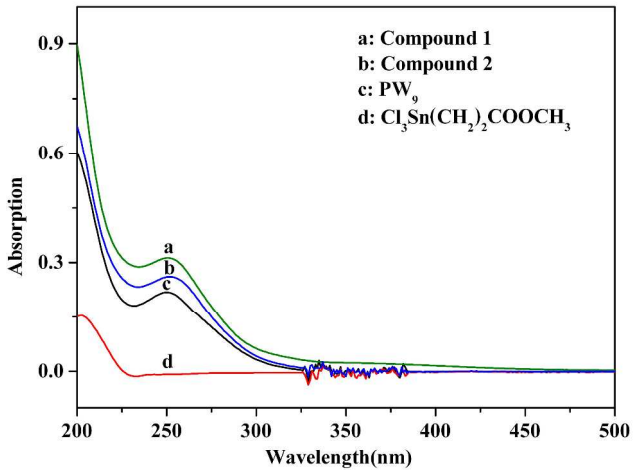

Fig. 2 The UV spectra of **1**, **2**, **PW₉** and $Cl_3Sn(CH_2)_2COOCH_3$

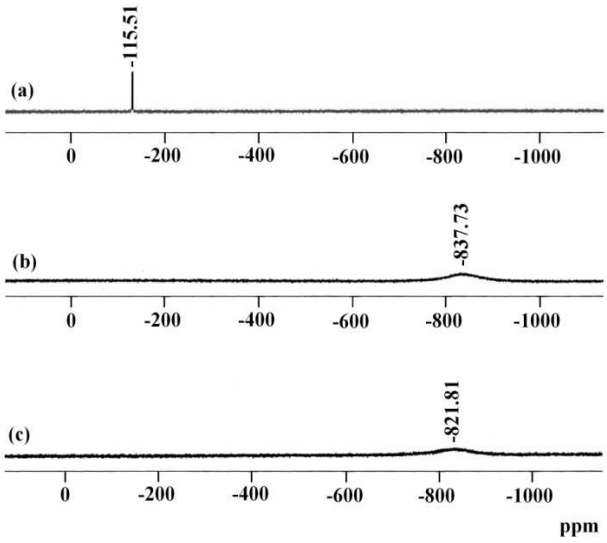

Fig. 3 The ^{119}Sn NMR spectra of $Cl_3Sn(CH_2)_2COOCH_3$ (a), compound **1** (b) and compound **2** (c)

35 to 653 °C, a three-continuous weight loss step is also observed (Fig. S8†). The total weight loss is 7.65% (Calc. 6.92%). Additionally, it can be seen from Figs. S7 and S8,† the TG curves rise slightly after about 660 °C, which may be caused by the oxidation process of tin in the air ambience.[22, 13c].

UV-Visible spectroscopy. The UV-vis absorption behaviours of **1**, **2** compared with **PW₉** and $Cl_3Sn(CH_2)_2COOCH_3$ were studied in an aqueous solution. As shown in Fig. 2, curves a and b, displaying a strong band emerged in the range of 230-260 nm, are similar to that of their parent compound **PW₉** (see curve c). The max absorbance at *ca*. 252, 253, and 249 nm for **1**, **2** and **PW₉** should be attributed to the characteristic absorption of POM, *i.e.* the oxygen to metal ($O_{bridging}\rightarrow W$) charge transfer.[16,23] The slightly red shifts of **1** and **2** were caused by the introduction of organotin groups.

Cyclic voltammetry (CV). The electrochemical properties of compounds **1** and **2** in pH = 3 (0.1 mol L^{-1} Na_2SO_4-H_2SO_4) solutions were studied by CV. As shown in Fig. S9,† only one cathode peak (−1257 mV) was observed in the range of 0 to −1500 mV for **1**. For **2**, in the potential range of 0 to –1500 mV,

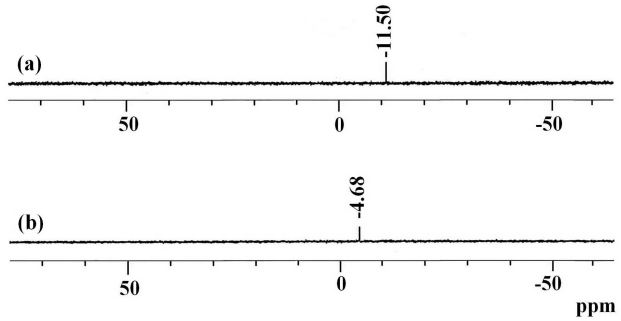

Fig. 4 The ^{31}P NMR spectra of starting material **PW₉-Zn** (a) and compound **2** (b)

there is one pair of redox peaks at E_{pa2} = –1254 mV, E_{pc2} = –1092 mV, ΔE_2 = 162 mV, and another one cathode peak at E_{pa1} = –687 mV (Fig. S10†), indicating the redox process of W^{VI}/W^{V} is irreversible. Furthermore, the peak potentials moved more negative direction compared with those of **PW₉-Mn** and **PW₉-Zn**.

NMR analysis. ^{119}Sn NMR and ^{31}P NMR spectra for **1**, **2**, and the original material $Cl_3Sn(CH_2)_2COOCH_3$, **PW₉-Mn/Zn** were performed to further confirm the organotin group was introduced into the POM skeleton and obtain more complete Keggin sandwich-type structural information. From the results shown in Figs. 3b and 3c, it is found that ^{119}Sn NMR with the chemical shifts at δ = –837.73 ppm (compound **1**) and δ = –821.81 ppm (compound **2**) obviously shifted to a higher field compared with that of $Cl_3Sn(CH_2)_2COOCH_3$ (δ = –115.51 ppm, Fig. 3a), due to the electron density on tin atom was increased. The result shows that the organotin group has been successfully incorporated into the POM system. In addition, ^{31}P NMR spectra for **PW₉-Zn** (δ = –11.50) and **2** (δ = –4.68 ppm) exhibit only one intense single peak (See Figs. 4a and 4b), demonstrating that the two symmetry-equivalent phosphorous atoms exist in the same chemical environments, which is consistent with the structural feature peaks of **PW₉** dimer. While for **1** and the starting material **PW₉-Mn**, no ^{31}P NMR signals were observed, such phenomena also appeared in some tungstophosphates containing Mn^{2+}. Perhaps the primary reason is that the ^{31}P NMR signal may be broadened by the incorporated paramagnetic manganese ions.[22, 24]

Fluorescence properties

The photoluminescence properties of **1**, **2** and the parent compound **PW₉-Mn/Zn** in the solid state at room temperature are depicted in Fig. 5. In order to investigate the electron transfer process between TiO_2 and compound **1**/**2**, the fluorescence spectra of **1-TiO₂**, **2-TiO₂**, **PW₉-Mn-TiO₂** and **PW₉-Zn-TiO₂** were also carried out. As shown in Fig. 5, the main emission peaks at 408, 470 nm for **1** and 416, 470 nm for **2** with λ_{ex} = 257 nm should be assigned to LMCT (O → W).[25] Compared with the emissions of the parents **PW₉-Mn** and **PW₉-Zn**, the maximum peak of **1** or **2** obviously red-shifts to the visible region. On the other hand, the emission intensity of **2** is higher than **1**. Excitingly, the emission of **1** or **2** with maximum peaks are very efficiently quenched after loaded TiO_2, see curves **1-TiO₂** and **2-TiO₂**. While for **PW₉-Mn-TiO₂** (see Fig. 5a) and **PW₉-Zn-TiO₂** (see Fig. 5b), the quenching phenomena do not appear. Thus the above results demonstrate that there exists a photoinduced electron transmission from **1**/**2** to TiO_2, that is to say, TiO_2 can extract the group enhanced the conjunction between POM and

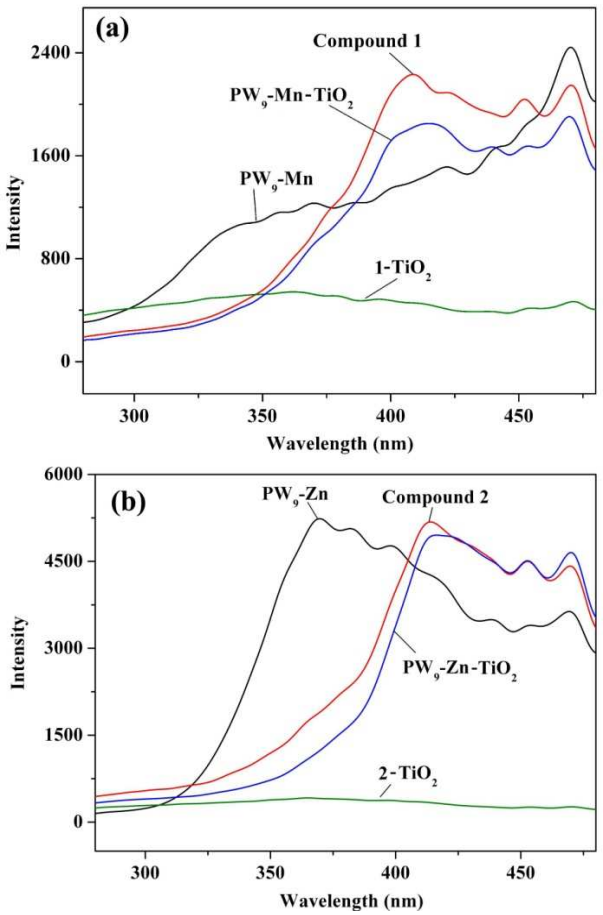

Fig. 5 Solid state emission spectra at room temperature. Comparison of compound **1**, **PW_9-Mn**, and effect of TiO_2 on their fluorescence emission spectra (a); Comparison of compound **2**, **PW_9-Zn**, and effect of TiO_2 on their fluorescence emission spectra (b)

TiO_2, which mean that the POM derivatives, **1** and **2**, may be excellent components of photocatalytic materials.

Catalytic activities

The electrocatalytic activities of compounds **1** and **2** toward the reduction of hydrogen peroxide in aqueous solution were studied. As shown in Fig. S11,† along with constantly adding H_2O_2, the cathodic currents obviously increase, while the relative anodic currents decrease. The results show that compound **1** has good electrocatalytic activity towards the selected elecrocatalytic reaction. While slight change in the cathodic current is observed for compound **2**-catalyzed reaction (Fig. S12†)**,** illustrating the electrocatalytic activity of the compound **2** is weaker than that of compound **1**.

Selecting the catalytic oxidation of cyclohexanol to cyclohexanone as a model reaction, and using aqueous hydrogen peroxide and compound **1**/**2** as oxidant and catalyst, respectively, the catalytic activity of compound **1/2** was studied. The catalytic performance was carried out according to our reported method and reaction conditions (80 °C, molar ratio of cyclohexanol to H_2O_2 is 1:2.2).[13c,26] Taking **PW_9-Zn** as an example, combining many factors from all sides, the affect of reaction time, the dosage of catalyst were systemically investigated. As shown in Fig. S13,† it is found that the yield of cyclohexanone slowly increased with the reaction time changed from 1.0 to 2.0 h, while further extending the reaction time to 2.5 h or 3.0 h, the cyclohexanone yield continuously decreased. As seen from Fig. S14,† it can be determined that the optimal amount of **PW_9-Zn** is 0.035 mmol, that is, the molar ratio of W/cyclohexanol is 1:150. On the basis of the above results, the optimum conditions for the catalytic oxidation of cyclohexanol to cyclohexanone were as follows: the reaction time is 2 h, and the molar ratios of the catalyst (based on W) to cyclohexanol and the cyclohexanol to H_2O_2 are 1:150 and 1:2.2, respectively, using 10 mL of acetonitrile as solvent at 80 °C. Subsequently, the catalytic activities of compounds **1**, **2**, **PW_9-Zn**, **PW_9-Mn** and $Cl_3Sn(CH_2)_2COOCH_3$ for the oxidation of cyclohexanol to cyclohexanone have been evaluated under the optimal reaction conditions. Compared with the parents, the as-prepared two compounds also exhibit good oxidation activity towards the target reaction (Table S3†). For example, the yields of cyclohexanol are 68.2% (compound **1**) and 73.8% (compound **2**), respectively. The above results argue that the organic-inorganic compounds **1** and **2** composed of carboxyltin group and transition metal modified polyoxometalates are excellent oxidation catalysts. Furthermore, we found that the catalytic activities of the obtained compounds unchanged after three repeated catalytic cycles (Fig. S15†). The actual catalysis could well be due to the formation of very small amounts of activated phosphotungstoperoxide complexes (Venturello complexes), which is a common occurrence in reactions of tungstophosphates with peroxide at elevated temperatures.[27]

Conclusions

Two new Keggin sandwich-type tungstenphosphates functionalized by transition metal ions and open-chain carboxyethyltin groups have been successfully synthesized in aqueous solutions. Compounds **1** and **2** display higher catalytic performances toward oxidation of cyclohexanol to cyclohexanone, and it can be reused three cycles without significant deactivation. The most significant is that **1**/**2**-TiO_2 exhibits very efficiently fluorescence quenching, which reflects the real role between POM and TiO_2, in other words, the arm-type polyoxometalates containing open-chain carboxyl groups maybe provide a good method to link POM and TiO_2. Accordingly, the introduced open-chain carboxyethyltin group will develop the application of the organotin-functionalized POM. We will continue to research the synthetic conditions and photoelectrochemical properties of a series of new arm-type POMs in our future work.

Acknowledgements

This work was financially supported by the Natural Science Foundation of Liaoning Province (no. 2013020128), the Foundation of Education Department of Liaoning Province (no. L2013414), the State Key Laboratory of Fine Chemicals of China (KF 1204) and the Key Laboratory of Polyoxometalate Science of Ministry of Education of China.

Notes and references

a School of Chemistry and Chemical Engineering, Liaoning Normal

University, Dalian 116029, China. E-mail: zhanglancui@lnnu.edu.cn; wsyou@lnnu.edu.cn; chemzhu@sina.com.
[b] *Center of Analytical Test, Liaoning Normal University, Dalian 116029.*

† Electronic Supplementary Information (ESI) available: Crystal structure figures, ORTEP views and packing views of **1** and **2**; selected bond lengths and angles, IR spectra, TG curves, PXRD patterns, CV curves, the optimal catalytic curves and and other supplementary materials. CCDC 1060303, 1060304. For ESI and crystallographic data in CIF or other electronic format. See DOI: 10.1039/b000000

1. (*a*) H. X. Yang, B. Q. Shan and L. Zhang, *RSC Adv*., 2014, **4**, 61226; (*b*) A. X. Yan, S. Yao, Y. G. Li, Z. M. Zhang, Y. Lu, W. L. Chen and E. B. Wang, *Chem. Eur. J*., 2014, **20**, 6927; (*c*) Y. F. Song and R. Tsunashima, *Chem. Soc. Rev*., 2012, **41**, 7384; (*d*) Y. Hou, L. N. Zakharov and M. Nyman, *J. Am. Chem. Soc*., 2013, **135**, 16651; (*e*) J. J. Stracke and R. G. Finke, *J. Am. Chem. Soc*., 2011, **133**, 14872.
2. (*a*) F. B. Xin, M. T. Pope, G. J. Long and U. Russo, *Inorg. Chem*., 1996, 35, 1207; (*b*) S. Reinoso, B. S. Bassil, M. Barsukova and U. Kortz, *Eur. J. Inorg. Chem*., 2010, **2010**, 2537.
3. F. B. Xin, M. T. Pope, *Organomet*., 1994, **13**, 4881.
4. L. F. Piedra-Garza, S. Reinoso, M. H. Dickman, M. M. Sanguineti and U. Kortz, *Dalton Trans*., 2009, 6231.
5. (*a*) H. Z. Liu, N. A. G. Bandeira, V. Félix and M. J. Calhorda, *Eur. J. Inorg. Chem*., 2013, **2013**, 1713; (*b*) S. Reinoso, M. H. Dickman, A. Praetorius, L. F. Piedra-Garza and U. Kortz, *Inorg. Chem*., 2008, **47**, 8798.
6. N. Belai and M. T. Pope, *Polyhedron*, 2006, **25**, 2015.
7. (*a*) C. Brazel, N. Dupré, M. Malacria, B. Hasenknopf, E. Lacôte and S. Thorimbert, *Chem. Eur. J*., 2014, **20**, 16074; (*b*) G. Geisberger, E. B. Gyenge, D. Hinger, P. Bösiger, C. Maakeb and G. R. Patzke, *Dalton Trans*., 2013, **42**, 9914; (*c*) N. Dupré, C. Brazel, L. Fensterbank, M. Malacria, S. Thorimbert, B. Hasenknopf and E. Lacôte, *Chem. Eur. J*., 2012, **18**, 12962; (*d*) C. Boglio, K. Micoine, E. Derat, R. Thouvenot, B. Hasenknopf, S. Thorimbert, E. Lacôte and M. Malacria, *J. Am. Chem. Soc*., 2008, **130**, 4553.
8. (*a*) X. H. Wang, H. C. Dai and J. F. Liu, *Polyhedron*, 1999, **18**, 2293; (*b*) V. H. Tran, T. P. Nguyen, P. Molinié, *Polym. Degrad. Stab*., 1996, **53**, 279.
9. L. J. Tian, Y. X. Sun, X. L. Zheng, X. C. Liu and B. C. Qian, *Chin. J. Inorg. Chem*., 2006, **22**, 629.
10. L. C. Zhang, H. Xue, Z. M. Zhu, Q. X. Wang, W. S. You, Y. G. Li and E. B. Wang, *Inorg. Chem. Commun*., 2010, **13**, 609.
11. G. Geisberger, E. B. Gyenge, D. Hinger, P.Bösiger, C. Maake and G. R. Patzke, *Dalton Trans*., 2013, **42**, 9914.
12. L. C. Zhang, S. L. Zheng, H. Xue, Z. M. Zhu, W. S. You, Y.G. Li and E. B.Wang, *Dalton Trans*., 2010, **39**, 3369.
13. (*a*) Z. J. Wang, L. C. Zhang, Z. M. Zhu, W. L. Chen, W. S. You and E. B. Wang, *Inorg. Chem. Commun*., 2012, **17**, 151; (*b*) H. Yang, L. C. Zhang, L. Yang, X. L. Zhang, W. S. You and Z. M. Zhu, *Inorg. Chem. Commun*., 2013, **29**, 33.
14. X. J. Sang, J. S. Li, L. C. Zhang, Z. J. Wang, W. L. Chen, Z. M. Zhu, Z. M. Su and E. B. Wang, *ACS. Appl. Mater. Interfaces*, 2014, **6**, 7876.
15. X. J. Sang, J. S. Li, L. C. Zhang,. Z. M. Zhu, W. L. Chen,. Y. G. Li, Z. M. Su and E. B. Wang, *Chem. Commun.,* 2014, **50**, 14678.
16. X. Y. Zhang, G. B. Jameson, C. J. O′Connor, and M. T. Pope, *Polyhedron*, 1996, **15**, 917.
17. H. T. Evans, C. M. Tourné, G. F. Tourné and T. J. R. Weakley, *J. Chem. Soc. Dalton Trans*., 1986, 2699.
18. R. E. Hutton, J. W. Burley and V. J. Oakes, *Organomet. Chem*., 1978, **156**, 369.
19. (*a*) G. M. Sheldrick, *SHELXL97, program for crystal structure refinement*, University of Gottingen, Germany, 1997; (*b*) G. M. Sheldrick, *SHELXS97*, *program for crystal structure solution*, University of Gottingen, Germany, 1997.
20. (*a*) T. T. Yu, H. Y. Ma, C. J. Zhang, H. J. Pang, S. B. Li and H. Liu, *Dalton Trans*., 2013, **42**, 16328. (*b*) K. Patel, B. K. Tripuramallu and A. Patel, *Eur. J. Inorg. Chem*., 2011, **2011**, 1871.
21. (*a*) M. K. Rauf, M. A. Saeed, Imtiaz-ud-Din, M. Bolte, A. Badshah and B. Mirza, *J. Organomet. Chem*., 2008, **693**, 3043. (*b*) J. W. Zhao, J. Zhang, Y. Song, S. T. Zheng and G. Y. Yang, *Eur. J. Inorg. Chem*., 2008, **2008**, 3809.
22. J. P. Bai, F. Su, H. T. Zhu, H. Sun, L. C. Zhang, M. Y. Liu, W. S. You and Z. M. Zhu, *Dalton Trans*., 2015, **44**, 6423.
23. (*a*) W. H. Knoth, P. J. Domaille, R. D. Farlee, *Organometallics,* 1985, **4**, 62. (*b*) R. Contant, *Can. J. Chem*., 1987, **65**, 568.
24. X. Zhang, Q. Chen, D. C. Duncan, R. J. Lachicotte and C. L. Hill, *Inorg. Chem*., 1997, **36**, 4381.
25. K. Stroobants, V. Goovaerts, G. Absillis, G. Bruylants, E. Moelants, P. Proost and T. N. Parac-Vogt, *Chem. Eur. J*., 2014, **20**, 9567.
26. C. Y. Yang, L. C. Zhang, Z. J. Wang, L. Wang, X. H. Li and Z. M. Zhu, *J. Solid State Chem*., 2012, **194**, 270.
27. (*a*) C Venturello and M Gambaro, *J. Org. Chem*., 1991, **56**, 5924; (*b*) C. Venturello, R. D'Aloisio, J. C. J. Bart and M. Ricci, *J. Mol. Catal. A*: *Chem.*, 1985, **32**, 107; (*c*) C. Venturello, E. Alneri and M. Ricci, *J. Org. Chem*., 1983, **48**, 3831; (*d*) M. K. Saini, R. Gupta, S. Parbhakar, S. Singh and F. Hussain, *RSC Adv.*, 2014, **4**, 38446; (*e*) H. Aoto, K. Matsui, Y. Sakai, T. Kuchizi, H.Sekiya, H. Osada, T. Yoshida, S. Matsunaga and K. Nomiya, *J. Mol. Catal. A*: *Chem*., 2014, **394**, 224, (*f*) D. C. Duncan, R. C. Chambers, E. Hecht and C. L. Hill, *J. Am. Chem. Soc*. 1995, **117**, 681.